SciVerse ScienceDirect

Procedia CIRP 9 (2013) 2 – 7

www.elsevier.com/locate/procedia

2nd CIRP Global Web Conference

Grinding of Iron-Aluminides

Jens Köhler[a], Analía Moral[a]*, Berend Denkena[a]

[a]*Institute of Production Engineering and Machine Tools, An der Universität 2, Garbsen 30823, Germany*

* Corresponding author. Tel.: +49-511-762-18002; Fax: +0049-511-762-5115; *E-mail address*: moral@ifw.uni-hannover.de

Abstract

Since the 1930s iron-aluminides are investigated due to their excellent corrosion resistance, low density and high specific strength. However, little work has been carried out on the machining of these alloys since then. This paper deals with grinding of Fe-26Al-4Cr (at.%) with corundum grinding wheels and shows that the material can be machined in a ductile way, regardless of the material grain size. Material removal rates below $Q'_w = 0.75$ mm³/mms and open grinding wheel topographies lead to low grinding temperatures and an advantageous chip removal. Thus, high process reliability regarding workpiece quality and tool wear can be reached.

Keywords: grinding; iron-aluminides; subsurface properties; surface roughness; subsurface hardness; grinding forces; grinding temperatures.

1. Introduction

1.1. Machining of iron-aluminides

Compared to conventional steel, iron-aluminides have excellent oxidation and corrosion properties, even at higher temperatures, a high specific strength and a high wear resistance [1, 2]. In addition, the raw materials and manufacturing costs of iron-aluminum alloys are relatively low. These properties offer a variety of applications in diverse fields, as for example their use as a heating material, as a structural material in the automotive industry or as a coating material for less corrosion-resistant substrate materials in the mining industry of fossil fuels [3, 4].

The low ductility of iron-aluminides, caused by embrittlement at room temperatures, as well as the low creep resistance and low strength at elevated temperatures (yield stress anomaly) limit their current application and make further development efforts necessary [2]. The use of additional alloying elements, such as chromium to increase ductility, was extensively studied in the past [5]. Alloying iron-aluminides with carbon to form the so-called κ-carbides was also investigated in order to influence the material microstructure and grain size [6] as well as recrystallization [7].

It was in 1961, while preparing some samples for tensile tests [8], when the poor machinability of these materials was first observed. A sharp milling cutter with a carbide-tip was used at slow speeds to produce tensile specimens. At first, satisfactory surface finish was reached, but the tools failed quickly due to the strong tendency of carbide tools to form a built–up edge at slow machining speeds. Woodyard [9] investigated the use of high-speed steel end mills to machine Fe28Al at.%, and found that it can be machined at speeds less than approx. 21 m/min. These tools allowed higher machining speeds than carbide end mills for comparable cutting environments. Woodyard determined that the effects of cutting temperatures also dominate lubrication effects at these cutting speeds. Saigal et al. [10] concluded, contrary to Woodyard, that high-speed steel tools cannot be used to machine iron-aluminides and rated the machinability of iron-aluminides at about 13.7, on a scale of 100. The cutting forces of iron-aluminides during milling are 1.5–3.5 times of those measured

doi:10.1016/j.procir.2013.06.158

during machining of medium carbon steels. The maximum cutting speed and depth of cut for the tool–workpiece combination are 60 m/min and 0.375 mm, respectively. Sasaki [11] showed that the tool life gradually decreased with increasing aluminum content and suggested a critical cutting speed of about 30 m/min for cemented carbide tools. Chowduri et al. [12] concluded that the cutting speed influences the chip formation mechanisms significantly, but not the tool life of coated and uncoated carbide tools. They attributed the accelerated wear on the tool flank during machining of iron-aluminides to thermal softening combined with abrasion.

Recent studies on turning of iron-aluminides [13] showed that the cutting speed and the tool material have a decisive influence on the wear mechanism. Due to the high strength of the material when subjected to pressure, the tool is subjected to high mechanical stress at low cutting speeds. This is reflected in the large cutting forces. The high process temperatures caused by the lower thermal conductivity of iron-aluminides lead to diffusion processes and increase the tribochemical wear. This mainly affects carbide tools. Coatings are recommended for cemented carbide cutting tools in order to protect them against thermal damage by forming a diffusion barrier. The abrupt changes in the mechanical properties as a function of grain orientation lead to an inhomogeneous chip formation, which is reflected in the changing chip thickness and shear angles, and thus in fluctuations in the process forces [13, 14].

Microcracks can occur during machining of FeAl (40 at.% Al) specimens [15]. These affect the mechanical properties of the alloy and can be attributed to environmental conditions during the cutting of alloys. Chao et al. [16] confirmed that the ductility of Fe40Al increased from 5% to 10% for imperfect to pre-polished samples. Morris [17] demonstrated the limited sensitivity of tensile ductility to preparation state. He proposed that not the roughness but the subsurface damage, caused by cracking and work hardening depending on machining depth, is responsible for the yield drop and tensile ductility. It leads to easier initiation of plastic deformation and to easier strain localization therefore to crack initiation. Additions of carbon to iron-aluminides, in the range of 0.1 to 1 wt%, allowed Prakash et al. to machine without surface cracking [18]. The improvement in machinability does not depend on amount or type (carbide or graphite) of second phase present, but may be related to a reduced susceptibility to hydrogen embrittlement, on account of the interstitial sites blocked by carbon in these alloys. Despite the mentioned improvements, the specimens still exhibited hydrogen embrittlement during subsequent tensile tests.

In order to manufacture products of iron-aluminides for the industry, an effective and economical workpiece finish is of great interest. High functional surface quality can be achieved by grinding, if the configuration of process parameters for the required workpiece quality is known. Only isolated findings [17] and some recent studies from the authors [19] deal with grinding of iron-aluminides. The aim of this work is to gain fundamental insights into the grinding of Fe-Al alloys with corundum grinding wheels. Material separation mechanisms are studied through single grain cutting tests. The grinding process parameters are based on these results. The influence of the grinding process on workpiece quality and tool wear is investigated for different grinding parameters.

2. Experimental setup and results

The interaction between one grain of the whole grinding wheel and material is hard to study during grinding, so that, first, single grain cutting tests on iron-aluminides were performed to observe the material removal mechanisms and cutting energy. Best suited parameters and tool specification can be identified through these experiments. To verify these results grinding experiments are also conducted.

2.1. Single grain cutting

2.1.1. Experimental setup

Table 1 shows the mechanical properties of the alloy. The tensile and compression tests were performed according to the standards EN 10002 and DIN EN 50125 - A 16 x 80, and the determination of the grain size according to DIN EN ISO 643 (intercepting method) at a magnification of 100:1. The Vickers hardness test corresponds to the DIN EN ISO 6507.

Table 1 Mechanical properties of Fe-26Al-4Cr (at. %)

Grain size	d_g	718 µm
Compressive yield	$R_{p0.2}$	625 MPa
Compressive strength	R_m	1434 MPa
Compressive failure	ε_{dB}	27.1 %
Tensile strength	R_m	263 MPa
Elongation	ε	0.18 %

A Fe-Al alloy with 26 at.% aluminum and 4 at.% chromium was used for all experiments. It has been selected in view of its improved strength and corrosion resistance in comparison with the binary alloys [7, 20]. The as-cast material has an average grain size of about 700 µm. The average material grain hardness is 347 HV.

The specimens were sawed in a rectangular form (Fig. 1). Their preparation through grinding and polishing has been carried out using different SiC grit sizes (800–1500) and water as a cooling and flushing medium. After that, the specimens were polished until Rz = 1 µm using ethanol-based lubricant. The surface of the specimens was later investigated through a Keyence optical microscope and was free of damage. The tests were carried out on the polished surface because of its more homogeneous grain size.

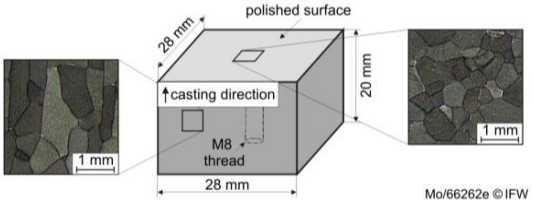

Fig. 1: Specimen for single grain cutting tests

The single grain cutting process (Fig. 2) has been carried out on a CNC profile grinding machine of the type Blohm Profimat 307. The used tools are cubic boron nitride (CBN) grains, which have a grain size of d_g = 250 µm, and have been soldered at a tip holder. An aluminum disk with a diameter of d_s = 400 mm has been used to hold the tools. The specimens have been mounted to a Kistler force sensor of the type 9117A 1.5 and horizontally positioned.

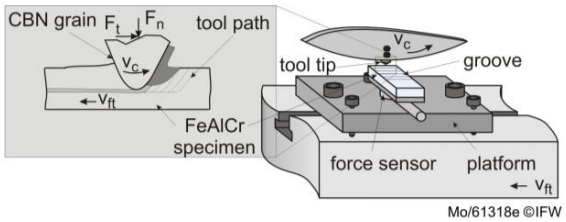

Fig. 2: Experimental setup for single grain cutting

The maximum single grain chip thickness h_{cumax} has been calculated by Malkin as follows [21]:

$$h_{cu\max.} \approx 2 \cdot \Pi \cdot d_s \cdot \frac{v_w}{v_s} \cdot \sqrt{\frac{a_e}{d_s}} - \Pi^2 \cdot d_s \cdot \left(\frac{v_w}{v_s}\right)^2 \qquad (1)$$

Whereas d_s is the diameter of the aluminum wheel, v_w the feed rate, v_s the cutting speed and a_e is the depth of cut per path.

2.1.2. Results

A ductile material separation mainly occurs at low cutting speeds v_c < 20 m/s, low tangential feed rates v_{ft} < 50 mm/min, and limited depth of cut per path (DOC) a_e up to 50 µm. However, the use of mineral oil is needed to produce a surface free of material outbreaks. A brittle material separation is also identified through cracks in the material surfaces, which are present in process configurations run over the limits pointed out above. Fig. 3 shows resulting grooves on Fe26Al4Cr (at. %) at different single grain chip thicknesses h_{cumax} (Eq. 1).

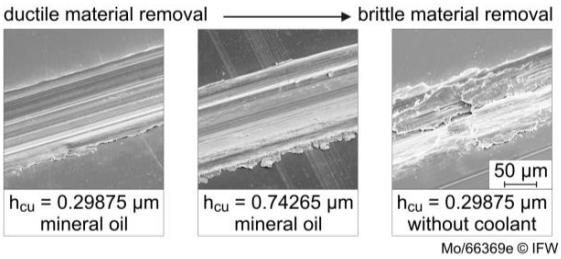

Fig. 3: Determination of material separation mechanisms by single grain cutting with CBN grains, $h_{cu} = h_{cumax}$

The SEM images in Figure 4 show that the main wear mechanisms, which occurred to the CBN grains, are breakouts, grain rupture and cutting edge chipping. Furthermore, material adhesions and grain flattening are observed at higher h_{cu}.

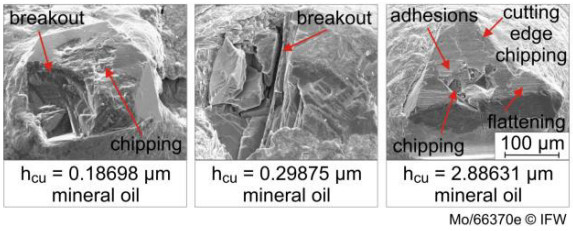

Fig. 4: Determination of wear mechanisms by single grain cutting with CBN grains, $h_{cu} = h_{cumax}$

The wear is caused by the low fracture toughness of the CBN cutting material and the dynamically changing process forces, which are due to changing material grain size and hardness [14]. Other reasons are fine microcracks in the grain structure which are already present prior to the experiments and act as a breaking point. Only some small material adhesions, which can be classified as diffusion, are determined by EDX analysis. A low diffusion wear of CBN tools under high thermal loads can be deduced from these results [13].

Analyzing the material removal coefficient f_{ab} and the specific cutting energy e_R (Fig. 5) it can be established that a single grain chip thickness h_{cu} between 0.29 µm and 0.73 µm produces a ductile material removal with smaller bulging area and minimum wear of CBN tools. For these $h_{cu,max}$-values are also calculated the lowest process energies, indicating a high efficiency of the machining process.

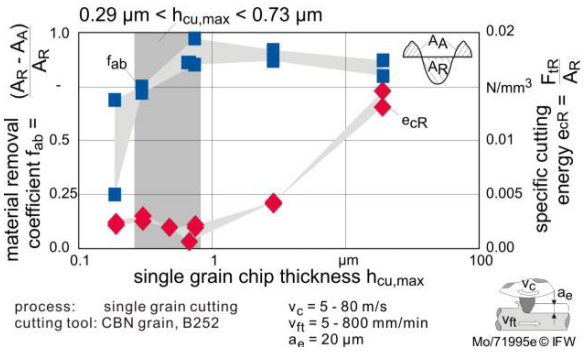

Fig. 5: Determination of material separation and wear mechanisms by scratch tests with CBN grains

Table 2 lists the settings for feed rate, cutting speed and depth of cut per path for the grinding tests. They were chosen to verify the results from single grain cutting but considering real process conditions, like for example limitations on the cutting speed regarding the grinding wheel type. The single grain tests showed that a_e > 50 µm leads to an increase of burr formation and tool wear, therefore in Table 2 a_e is set to 50 µm while varying the feed rate v_{ft} and the cutting speed v_c.

Table 2: Grinding process parameters

Eq. single grain chip thickness h_{eq} [mm]	Feed rate v_{ft} [mm/min]	Cutting speed v_c [m/s]	DOC a_e [µm]
$6.25x10^{-6}$ – $5.00x10^{-5}$	300 - 2400	40	50
$5.00x10^{-5}$ – $1.25x10^{-5}$	600	10 - 40	50
$6.25x10^{-6}$ – $2.5x10^{-5}$	600	40	25 - 100

The equivalent chip thickness h_{eq} is calculated by replacing the grinding parameters listed in Table 2 in Eq. 2 [21, 22, 23]:

$$h_{eq} = \frac{v_{ft}}{v_c} \cdot a_e \quad (2)$$

To obtain h_{cu} for grinding the substitute cutting depth z_e is calculated from Eq. 3 by using h_{eq} values listed in Table 2. Considering that the grains have a round cross section are $C_1 = 10.6$ and $C_2 = 1.5$. The contact length is $l_g = 3.87$ mm for a grinding wheel with a diameter $d_s = 300$ mm. The number of grains per unit volume is $N_v = 28.67$ 1/mm³ for a grain size of CBN $d_{gCBN} = 250$ µm.

$$z_e = \left(\frac{(c_2+1)}{N_V \cdot c_1} \cdot \frac{h_{eq}}{l_g} \right)^{\left(\frac{1}{c_2+1}\right)} \quad (3)$$

This results in a substitute cutting depth z_e of about: $0.7\mu m \le z_e \le 1.6\mu m$.

Replacing z_e in Eq. 4 to calculate h_{cu} for grinding [24] results in h_{cu} values of about: $0.38\mu m \le h_{cu} \le 0.88\mu m$.

$$h_{cu} = \left(\frac{1}{c_2+1} \right)^{\left(\frac{1}{c_2}\right)} \cdot z_e \quad (4)$$

A corundum grinding wheel with a grain size of about $d_g = 250$ µm and vitrified bond was chosen for the grinding tests. This ensures sufficient chip space. It must be noticed that the single grain chip thickness h_{cu} and the equivalent chip thickness h_{eq} are much smaller than the material grain size (see Table 2). Therefore the influence of the material grain size and orientation may not have a strong influence on the results as it does during cutting. Examples of chip formation during grinding were demonstrated by [24]. Since CBN is a super abrasive, it is possible to compare the single grain chip thickness from single grain cutting h_{cu-max} with the single grain chip thickness h_{cu} from grinding with corundum. However, regarding tool wear, workpiece temperature and workpiece quality bigger specific material removal rate Q'$_w$ are expected while grinding with CBN than while grinding with corundum.

2.2. Grinding

2.2.1. Experimental setup

The grinding machine Blohm Profimat 307 was also used for the grinding investigations (Fig. 6). The evaluation of the dressing and grinding process is carried out by the grinding forces F_n and F_t and the grinding temperatures at a depth of about 50 µm from the contact zone T_{k50}. In order to measure the process forces a 3-component dynamometer Type 9257B by Kistler was used. For the investigation of the grinding temperature flat specimens with integrated thermocouples model Ni-Cr-Ni (K) accuracy class 1 were used.

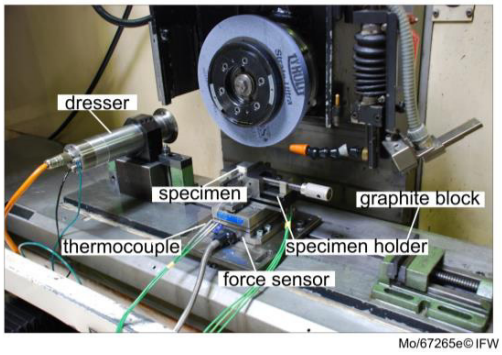

Fig. 6: Experimental setup for grinding

The grinding wheel topography was examined with an optical microscope before and after each grinding test so that possible changes, such as attachments or break outs, can be investigated. Since during grinding a half of

the grinding wheel width was in contact with the workpiece, the radial wear was measured by grinding of graphite plates. The evaluation of the graphite plates was performed using the contour measuring machine Perthometer Concept by Mahr. The surface roughness Rz, SEM images of the grinding marks, as well as micrographs and micro-hardness measurements of the marginal zone were interpreted as indicators of the work-piece quality.

2.2.2. Results

The dressing process has a significant effect on the grinding results [26]. Grinding wheel topographies with low actual surface roughness lead to high thermomechanical loads on the workpiece, and consequently damage its surface and subsurface. Therefore a rough grinding wheel topography is recommended to grind Fe-26Al-4Cr (at. %) (Fig. 7).

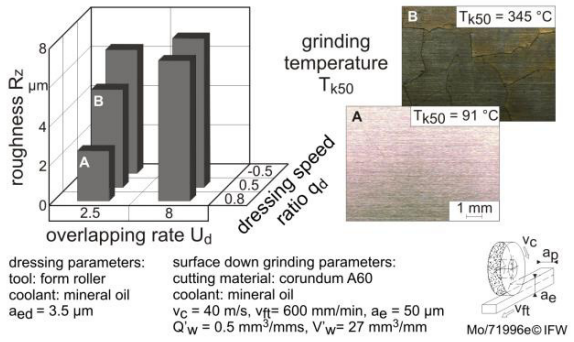

Fig. 7: Influence of dressing process configuration on grinding results

Figure 8 shows that a material removal rate of $Q'_w = 0.75$ mm³/mms can be achieved without damage of the workpiece ($T_{k50} < 200$ °C), when grinding with a corundum grinding wheel. Work-related workpiece-damage at higher removal rates is mainly caused by the higher thermal workpiece loads. Grinding temperatures of $T_{k50} > 220$ °C generally result in workpiece damage. The experimental investigations show that the workpiece damage is rather caused by grinding temperatures than by mechanical loading. This can be observed in Fig. 8, where the specific grinding force F'_n doesn't rise as the process temperature T_{k50} does.

A higher influence of the depth of cut on the grinding temperature than the feed speed is already known for other materials like steel [27]. The much higher contact zone temperature during creep feed grinding, however, is based not only on the larger tangential force, but also to the larger contact area between the grinding wheel and the workpiece and the associated poor coolant flow and insufficient chip evacuation. The cutting speed has only a small influence on the grinding temperature, since it largely compensates factors that increase or reduce temperature. A rise in the cutting speed leads to a reduction of the radial forces and wear, and to an improvement of the workpiece surface quality. Machining at cutting speeds higher than $v_c > 10$ m/s is therefore recommended.

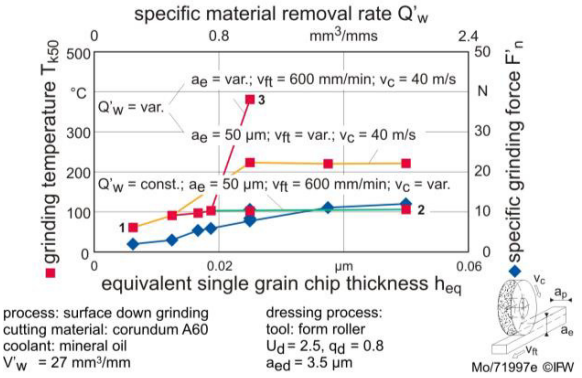

Fig. 8: Influence of the setting on the grinding temperatures and forces

The radial tool wear was for all experiments $\Delta r < 5$ µm. It was observed that at material removal rates higher than $Q'_w > 0.75$ mm³/mms and at lower cutting speeds of $v_c \leq 20$ m/s material adhesions occur on the grinding wheel topography clogging it up.

Through grinding the subsurface zone properties are affected. Figure 9 shows a representative SEM analysis of the surface topography (top) and the metallographic cross sections (bottom), and the corresponding surface roughness Rz and subsurface hardness measured at the respective depth z = 100 µm (z_{100}) and z = 1000 µm (z_{1000}).

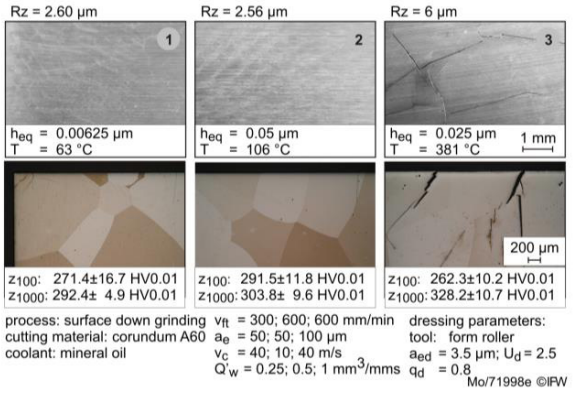

Fig. 9: Workpiece surface and subsurface analysis

The SEM and the cross-sectional images demonstrate that the cracks occur in the surface and in the subsurface zone at higher grinding temperatures. The average hardness values in the subsurface are calculated from ten measurements. The hardness of the subsurface zone

shows a strong difference to the hardness of the bulk material, see example for specimen 3. Specimens 1 and 2 show no significant effect of treatment on the hardness in the surface layer. From these results it can be concluded that the single grain chip thickness is not relevant to the surface and subsurface quality of the component, but workpiece damage can be caused by higher grinding temperatures.

3. Summary and outlook

This work deduced the main characteristics of grinding tools and the grinding process configuration for Fe26Al4Cr (at. %) from single grain cutting tests. Ductile material removal mechanisms and smaller tool wear were observed during single cutting with CBN grains and mineral oil as coolant at the single grain chip thickness of about $0.29\ \mu m < h_{cu\text{-}max} < 0.73\ \mu m$. Comparable h_{cu} values for grinding were calculated from suitable grinding parameters. Grinding force and temperature as well as workpiece quality were evaluated to verify the results. By using $h_{cu\text{-}max}$ values derived from single grain cutting it is possible to set adequate grinding parameters. The specific material removal rate was limited to $Q'_w = 0.75\ mm^3/mm.s$ principally by the grinding depth of cut of ae = 75 µm. Further improvements in the grinding process are proposed by the authors by reducing the tool grain size, which leads to a smaller single grain chip thickness, and by using CBN grinding wheels, which reduces the contact zone temperature and shows higher resistance to tool wear than corundum grinding wheels.

Acknowledgements

The authors would like to thank the German Research Foundation (DFG) for the economic support during the research project DE-447/62-1 “Grinding of Iron-Aluminides”.

References

[1] Alman, D. E., Hawk, J.A., Tylczak, J.H., 2001. Wear of Iron-Aluminide Intermetallic-Based Alloys and Composites by Hard Particles, Wear 251 (1-12), p. 875-884.

[2] Stoloff, N. S., 1998. Iron-aluminides: Present Status and Future Prospects, Materials science and engineering A 258 (1-2), p. 1-14.

[3] Totemeier, T. C., Wright, R. N., Swank, W. D., 2003. Mechanical and Physical Properties of High-velocity Oxy-fuel-sprayed Iron Aluminide Coatings, Metallurgical and Materials Transactions 34 A (10), p. 2223-2231.

[4] Deevi, S. C., Sikka, V. K., 1996. Nickel and iron-aluminides: An Overview on Properties, Processing, and Applications, Intermetallics 4 (5), p. 357-375.

[5] McKamey, C. G., Horton, J. A., Liu, C. T., 1989. Effect of Chromium on Properties of Fe3Al, Journal of Materials Research 4 (5), p. 1156-1163.

[6] Schneider, A., Falat, L., Sauthoff, G., 2005. Microstructures and Mechanical Properties of Fe3Al-based Fe–Al–C Alloys, Intermetallics 13 (12), p. 1322-1331.

[7] Kobayashi, S., Zaefferer, S., 2008. Determination of Phase Equilibria in the Fe3Al-Cr-Mo-C Semi-quaternary System Using a New Multiple-diffusion Technique, Journal of Alloys and Compounds 452 (1), p. 67-72.

[8] Holladay, J. W., 1961. Review of Development in Iron-Aluminum-Base Alloys, DMIC Memo 82. Columbus, OH: Defense Metals Information Center, Battelle Memorial Institute

[9] Woodyard, J. R., 1992. Machining of Fe_3Al Intermetallics, Report of investigations, Washington, D. C.: U. S., Dept. of Interior, Bureau of Mines.

[10] Saigal, A., Yang, W., 2003. Analysis of Milling of Iron-Aluminides, Journal of Materials Processing Technology 132 (1-3), p. 149 - 156.

[11] Sasaki, T., & Yako, T., 2004. Influence of Aluminum Content on Machinability of Intermetallic FeAl. Nihon Kikai Gakkai Seisan Kako, Kosaku Kikai Bumon Koenkai Koen Ronbunshu 5, p. 171-172.

[12] Chowdhuri, S., Joshi, S. S., Rao, P. K., Ballal, N.B., 2004. Machining Aspects of a High Carbon Fe3Al Alloy, J. Mater. Proc. Technol. 147, p. 131–138.

[13] Denkena, B., Reichstein, M., Meyer, R., 2006. Spanen von Eisen-Aluminium-Legierungen, Tribochemsiche Verschleiß-mechanismen beim Drehen intermetallischer Eisen-Aluminium-Legierungen, wt Werkstatttechnik online 96 (11-12), p. 798-804.

[14] Denkena. B., Reichstein, M., Meyer, R., 2007. Interactions and Causes for Tool Wear in Machining Intermetallic FeAl-Alloys, Sixth International Conference on High Speed Machining, 21-22 March, San Sebastián, Spain, Proc. auf CD-ROM.

[15] Ferguson, P. A., Liu, C. T., 1992. Cracking behavior of FeAl (40 at. % Al) alloys during cutting operations, Scripta Metallurgica et Materialia 26 (11), p. 1669-1674.

[16] Chao, J., Morris, D.G., Muñoz-Morris, M.A., Gonzalez-Carrasco, J.L., 2001. The Influence of some Microstructural and Test Parameters on the Tensile Stress and Ductility Behaviour of a mechanically-alloyed FeAl, Intermetallics 9 (4), p. 299-308.

[17] Morris, D.G., Garcia Oca, C., Chao, J., Muñoz-Morris, M.A., 2002. Influence of Machining Conditions on Tensile Stress and Ductility of a Mechanically alloyed Fe–40Al intermetallic, Scripta Materialia 46 (12), p. 843–850.

[18] Prakash, U., Sauthoff, G., 2001. Machinable Iron-Aluminides Containing Carbon, Scripta Materialia. 44 (1), p. 73–78.

[19] Denkena, B., Meyer, R., Stiffel, J.-H., Moral, A. I. 2011. Machining of Iron-Aluminum Alloys, AMST'11, Mali Losinj, Croatia, p. 76-89.

[20] Regina, J. R., DuPont, J. N., Marder, A. R., 2005. Gaseous Corrosion Resistance of Fe-Al-based Alloys Containing Cr Additions. Part I: Kinetic results, Materials Science and Engineering A, 404 (1-2), p. 71-78.

[21] Malkin, S., 1989. Grinding Technology: Theory and Application of Machining with Abrasives, John Wiley & Sons, New York, Dearborn: Reprinted by SME.

[22] Zum Gahr, K.-H., 1981. Abrasive wear of Metallic Materials, Progress Reports of the VDI Journals, 5 (57), VDI-Verlag, Düsseldorf.

[23] Denkena, B., Tönshoff, H. K., 2011. Spanen - Grundlagen, 3rd Revised and Extended Edition, Springer-Verlag, Berlin, Heidelberg.

[24] Degner, W. Lutze, H., Smejkal, E., 2009. Spanende Formung, Theorie-Berechnung-Richtwerte, Carl Hanser Verlag, München.

[25] Denkena, B., Köhler, J., Kästner, J., 2012. Chip formation in grinding: an experimental study, Production Engineering 6 (2), p. 107-115.

[26] Klocke, F., Linke, B., 2008. Mechanisms in the generation of grinding wheel topography by dressing, Production Engineering 2 (2), p. 157-163.

[27] Brandin, H., 1978. Pendelschleifen und Tiefschleifen: Vergleichende Untersuchungen beim Schleifen von Rechteckprofilen. Doctoral Thesis, Technische Universität Carolo-Wilhelmina zu Braunschweig.